Article

Functionalization and Coordination Effects on the Structural Chemistry of Pendant Arm Derivatives of 1,4,7-trithia-10-aza-cyclododecane ([12]aneNS$_3$)

Claudia Caltagirone [1], Maria Carla Aragoni [1], Massimiliano Arca [1], Alexander John Blake [2,*], Francesco Demartin [3], Alessandra Garau [1], Enrico Podda [4], Alexandra Pop [5], Vito Lippolis [1,*] and Cristian Silvestru [5]

[1] Dipartimento di Scienze Chimiche e Geologiche, Università degli Studi di Cagliari, S.S. 554 Bivio per Sestu, 09042 Monserrato (CA), Italy
[2] School of Chemistry, University of Nottingham, University Park, Nottingham NG7 2RD, UK
[3] Dipartimento di Chimica, Università degli Studi di Milano, 20133 Milano, Italy
[4] Centro Servizi di Ateneo per la Ricerca-CeSAR, Università degli Studi di Cagliari, S.S. 554 Bivio per Sestu, 09042 Monserrato (CA), Italy
[5] Supramolecular Organic and Organometallic Chemistry Centre, Department of Chemistry, Faculty of Chemistry and Chemical Engineering, Babes-Bolyai University, Str. Arany Janos 11, 400028 Cluj-Napoca, Romania
* Correspondence: alexander.blake@ntlworld.com (A.J.B.); lippolis@unica.it (V.L.)

Abstract: The effect of different pendant arms on the structural chemistry of the 1,4,7-trithia-10-aza-cyclododecane ([12]aneNS$_3$) macrocycle is discussed in relation to the coordination chemistry of all known functionalized derivatives of [12]aneNS$_3$, which have been structurally characterized.

Keywords: 1,4,7-trithia-10-aza-cyclododecane; macrocyclic ligands; pendant arms; conformation

1. Introduction

1,4,7-Trithia-10-aza-cyclododecane ([12]aneNS$_3$ (**L** in Figure 1) is a well-known 12-membered mixed thia-aza macrocycle featuring a NS$_3$ donor set suitable for coordination to soft metal ions [1–15]. It has been extensively functionalized at the secondary nitrogen atom to afford pendant arm derivatives for different purposes: fluorescent materials and chemosensors for heavy metal ions [3,4,9–11], highly selective heteroditopic ionophores for simultaneous binding, extraction and transport of both the cationic and anionic moieties of toxic and/or precious transition metal salts [12,13], crystal engineering in the preparation of coordination polymers [5,8,12], tuning of the coordination environment around soft metal ions [2,6,7,15], and development of new synthetic methods of mixed-donor thiacrown ethers [1,14]. All structurally characterized pendant arm derivatives of [12]aneNS$_3$ (**L**) are reported in Figure 1, including both metal-coordinated ligands (drawn in black) and free ligands (drawn in red). Of note, no X-ray crystal structure of **L** is known, and **L7** is the only derivative of [12]aneNS$_3$ for which the X-ray crystal structure is known together with some of its transition metal coordination compounds. In this paper, we report the X-ray crystal structure of **L12** and the synthesis and structural characterization of two new **L** derivatives, i.e., **L20** and **L21**·CHCl$_3$ (Figure 2). The two new derivatives of **L** were chosen to favor intermolecular interactions involving the functional groups in the pendant arm and the donor atoms from the macrocyclic moiety. In particular, in the case of **L20,** we wanted to explore the possibility of intermolecular halogen bonds (XBs) formation involving the S donor atoms of the macrocyclic moiety and the effects on its conformation. The three new crystal structures are discussed and compared with those already known in order to identify particular trends in the conformational changes in the macrocyclic moiety upon

coordination with metal ions, and the geometrical effects induced by pendant arms bearing additional functionalities.
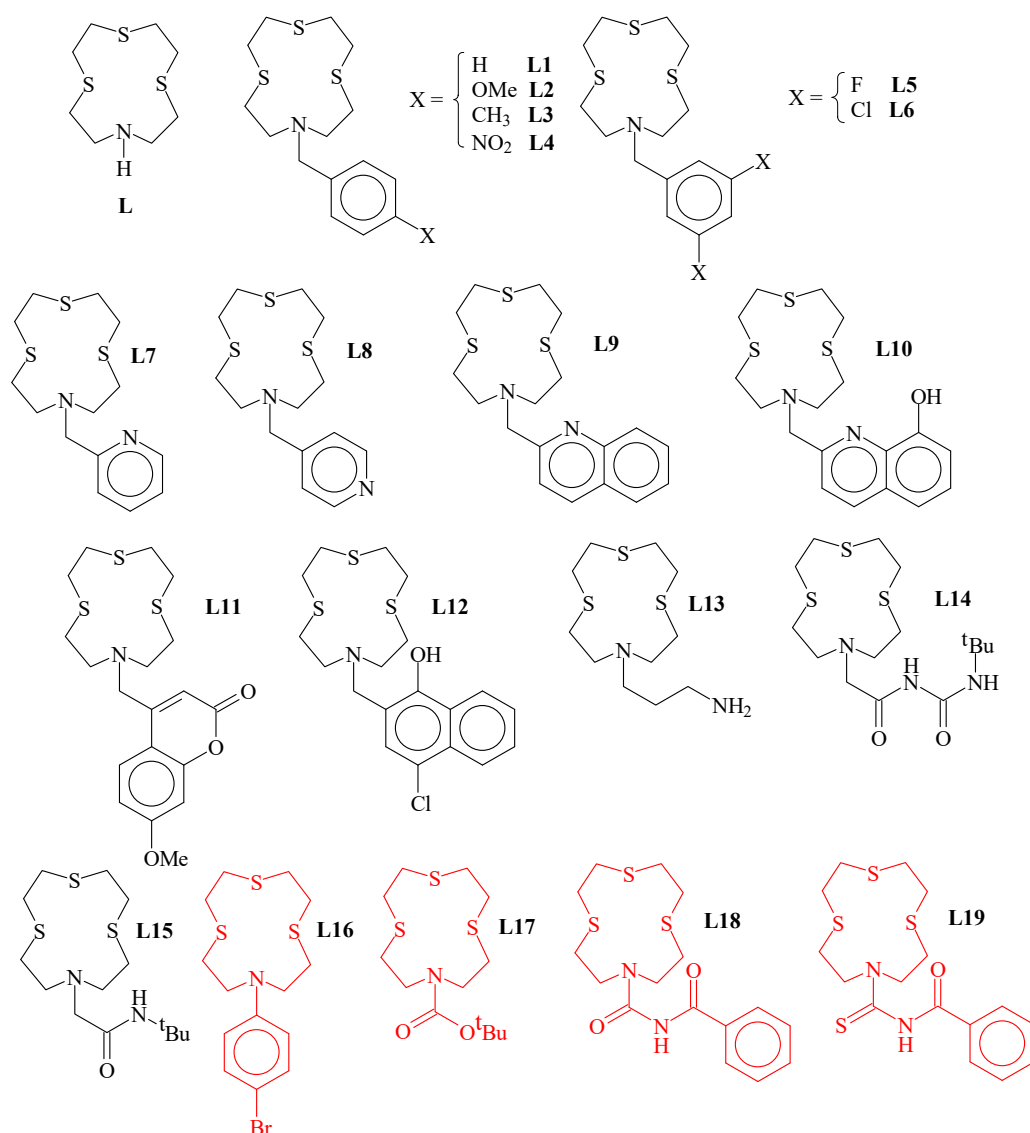

Figure 1. Summary of the crystallographically characterized [12]aneNS$_3$ (**L**) derivatives reported in the Cambridge Structural Database (CSD accessed on 13 January 2023) either as metal-coordinated ligands (drawn in black) or as free ligands (drawn in red). [**LH**]Br·2H$_2$O [1]; [Cd(**L**)(NO$_3$)$_2$] [2]; [{Tl(**L**)}$_2${Au(C$_6$Cl$_5$)$_2$}][Au(C$_6$Cl$_5$)$_2$], [{Tl([**L**)}{Au(C$_6$F$_5$)$_2$}]$_2$ [3]; [{Ag(**L**)}{Au(C$_6$F$_5$)$_2$}]$_2$ [4]; {[Ag(**L1**)](OTf)·MeCN}$_\infty$, {[Ag(**L2**)](PF$_6$)·MeCN}$_\infty$, {[Ag(**L3**)](OTf)·MeCN}$_\infty$, [Ag$_3$(**L4**)$_3$](OTf)$_3$·4MeCN, {[Ag(**L5**)](OTf)·Me$_2$CO}$_\infty$, [Ag$_3$(**L6**)$_3$](OTf)$_3$·2MeOH·H$_2$O [5]; **L7**, [Hg(**L7**)][HgCl$_4$], [Cd(**L7**)I][CdI$_4$] [6]; [Mo(CO)$_3$(**L7**)] [7]; [Ag$_2$(**L7**)$_2$](OTf)$_2$·2MeCN, [Ag$_2$(**L8**)$_2$](OTf)$_2$·2MeCN [8]; [Ag(**L9**)][Au(C$_6$F$_5$)$_2$]·THF, [{Au(C$_6$F$_5$)$_2$}$_2$Ag$_2${Au(C$_6$F$_5$)$_2$}$_2${Ag(**L9**)}$_2$]·2THF [4]; [Zn(**L10**)](ClO$_4$)$_2$ [9]; [Hg(**L11**$_{-H}$)](NO$_3$) [10]; [Zn(**L12**)$_2$H$_2$O](BF$_4$)$_2$ [9]; [Hg(**L13**)](ClO$_4$)$_2$ [11]; [CuCl(**L14**)][CuCl$_4$], {[Ag(**L14**)](NO$_3$)}$_\infty$ [12]; {[Ag(**L15**)](NO$_3$)}$_\infty$ [13]; **L16** [14]; **L17** [15]; **L18**, **L19** [13].
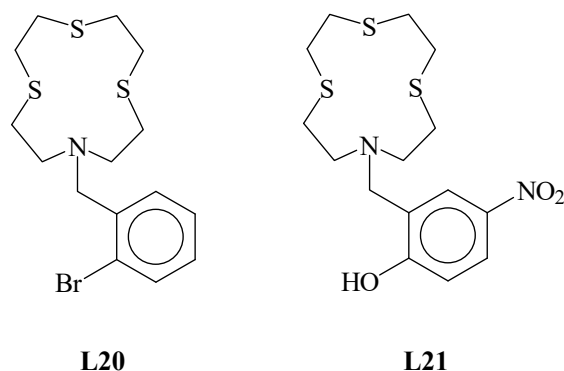
L20   **L21**

Figure 2. New pendant arm derivatives of **L** discussed in this paper.

2. Materials and Methods

2.1. Materials and Methods

1,4,7-Trithia-10-aza-cyclododecane ([12]aneNS$_3$) [11] and **L12** were synthesized according to the procedure reported in the literature [9]. Reagents and solvents were used that were purchased from Aldrich. Elemental analyses were performed with an EA1108 CHNS-O Fisons instrument (*T* = 1000 °C). The ^{1}H- and ^{13}C-NMR spectra were determined on a Bruker Avance 600 MHz spectrometer. The mass spectra were recorded on a triple quadrupole QqQ Varian 310-MS mass spectrometer by using the atmospheric pressure ESI technique. All sample solutions were infused into the ESI source with a programmable syringe pump (1.50 mL/h constant flow rate). A dwell time of 14 s was used, and the spectra were accumulated for at least 10 min to increase the signal-to-noise ratio. The mass spectra were recorded in the *m/z* 100−1000 range. The following scan parameters were chosen [16]: needle voltage 3500 V, shield 800 V, source temperature 60 °C, drying gas pressure 20 psi, nebulizing gas pressure 20 psi, detector voltage 1450 V, and drying gas temperature 110 °C. The isotopic patterns of the measured peaks in the mass spectra were analyzed using the mMass 5.5.0 software package [17]. All mass values were indicated as monoisotopic masses, which were computed as the sum of the masses of the primary isotope of each atom in the molecule (note that the monoisotopic mass may differ from the nominal molecular mass).

2.2. X-ray Diffraction Analyses

Only special features are noted here. Crystallographic data are reported in Table S1 in the Supplementary Materials. Single-crystal X-ray diffraction (SC-XRD) data for compound **L12** were collected at 150 K on a Bruker SMART 1000 diffractometer using MoKα radiation. The data were indexed and processed using Bruker SAINT and SMART [18,19]. The structure was solved by the SIR92 [20] solution program using direct methods. SC-XRD data for compound **L20** were collected at 293 K on an Agilent SuperNova diffractometer equipped with an Eos detector using MoKα radiation. The data were indexed and processed using CrysalisPro [21] and the structure was solved by SHELXT [22] using dual-space methods. SC-XRD data for the compound **L21**·CHCl$_3$ were collected at 293 K on a Bruker APEX II CCD diffractometer using MoKα radiation. The data were indexed and processed using Bruker SAINT [18]. The structure was solved by SIR92 [20] using direct methods. The models were refined with ShelXL [23] using full-matrix least-squares minimization on F^2. All non-hydrogen atoms were anisotropically refined. Hydrogen atom positions were geometrically calculated and refined using the riding model. Olex2, version 1.5 [24], was used as the graphical interface. For the compound **L21**·CHCl$_3$, the solvent molecule was disordered and modelled over two sites with statistically the same occupancy [0.49(1) and 0.51(1), respectively]. Complete crystallographic data for the structure of compounds **L12**, **L20**, and **L21**·CHCl$_3$ were deposited in CIF format at the Cambridge Crystallographic Data Center (CCDC) with deposition numbers 2248158-2248160, respectively.

2.3. Synthesis of L20

A mixture of 1,4,7-trithia-10-aza-cyclododecane (0.178 g, 0.790 mmol), 2-bromobenzyl bromide (0.199 g 0.790 mmol), and K_2CO_3 (0.37 g, 2.6 mmol) in dry MeCN (50 mL) was heated to reflux for 96 h under a dry N_2 atmosphere. The solid was filtered off and the solvent was removed under reduced pressure. The residue was dissolved in dichloromethane (DCM) and washed with distilled water. The organic phase was dried over Na_2SO_4 and the solvent was removed under reduced pressure. The residue was purified by flash chromatography (silica) using DCM/MeOH (10:0.3, *v/v*) as eluent to give a pale-yellow solid (0.187 mg, 0.63 mmol, 80% yield). **Elemental analysis, Found (Calcd. for $C_{15}H_{22}BrNS_3$):** C, 45.68 (45.91); H, 5.58 (5.65); N, 3.71 (3.57); S, 24.42 (24.51)%. M.p. 108 °C; ^{1}H-NMR (CDCl$_3$, 600 MHz): δ$_H$ (ppm) 2.65–2.69 (m, 4H), 2.78–2.82 (m, 12H), 3.71 (s, 2H, NC*H$_2$*Ar), 7.12 (t, *J* = 7.1 Hz, 1H), 7.29 (t, *J* = 7.3 Hz, 1H), and 7.54 (d, *J* = 7.5 Hz, 2H); ^{13}C{^{1}H}-NMR (CDCl$_3$, 150 MHz): δ$_C$ (ppm) 25.90, 27.86, 28.49 (CH$_2$S), 51.86 (CH$_2$N), 59.55 (NCH$_2$Ar), 124.38, 127.41, 129.70, 130.69, 132.85, and 137.88 (aromatic carbons); and ESI-MS(+): *m/z* = 393 [M+H]$^+$. The crystals of **L20** suitable for an X-ray diffraction analysis were grown from a DCM solution by diffusion of Et$_2$O vapor.

2.4. Synthesis of L21

A weighted amount of 2-hydroxy-5-nitrobenzyl bromide (0.170 g, 0.740 mmol) was added to a solution of 1,4,7-trithia-10-aza-cyclododecane (0.150 g, 0.670 mmol) and K_2CO_3 (0.460 g, 3.33 mmol) in dry MeCN (20 mL). The reaction mixture was heated under nitrogen at 80 °C for 24 h and then for 24 h at room temperature. The solid was filtered off, and the solvent was removed under reduced pressure to give a yellow solid (0.170 mg, 0.45 mmol, 68% yield). **Elemental analysis, Found (Calcd. for $C_{15}H_{22}N_2O_3S_3$):** C, 48.51 (48.10);H, 6.12 (5.92); N, 7.48 (7.48); S, 25.91 (25.68)%. M.p. 175 °C; ^{1}H-NMR (CDCl$_3$/CD$_3$CN, 600 MHz): δ$_H$ (ppm) 2.68 (m, 4H), 2.76 (m, 8H), 2.81 (m, 4H), 3.71 (s, 2H, NC*H$_2$*Ar), 6.56 (d, *J* = 9.2 Hz, 1H), 7.91 (dd, *J* = 3.0 Hz, 1H), and 8.05 (d, *J* = 2.8 Hz, 1H); ^{13}C{^{1}H}-NMR (CDCl$_3$/CD$_3$CN, 150 MHz): δ$_C$ (ppm) 26.5, 29.2, 29.4(CH$_2$S), 52.5 (CH$_2$N), 56.1 (NCH$_2$Ar), 118.7, 126.2, 126.9, 127.4, 136.7, and 172.6 (aromatic carbons); and ESI-MS(+): *m/z* = 375 [M+H]$^+$. The crystals of **L21**·CHCl$_3$ suitable for an X-ray diffraction analysis were grown from a CHCl$_3$ solution.

3. Results and Discussion

The X-ray crystal structure of **L12** is characterized by the formation of dimeric arrangements via N···H–O hydrogen bonds involving the –OH group and the aromatic N atom from the pendant arms of two symmetry-related ligand units (Figure 3). π-π Stacking interactions between the quinoline moieties of adjacent slipped dimers (centroid-centroid distance: 3.77 Å) generate a staircase architecture along the *b*-axis as shown in Figure S1 in the Supplementary Materials.

In **L12**, the macrocyclic unit adopts a square-shaped conformation with the four donor atoms occupying the corners. A useful convention to describe the different conformations that an aliphatic macrocycle can adopt is that of Dale [25], and it is based on the sequence of torsion angles around the macrocycle ring, which normally are classified as either *anti* (≅180°) or *gauche* (≅60°). According to the Dale convention, a generic conformation is determined by the number of bonds between each corner in the macrocycle (a corner is the atom at which two *gauche* torsion angles intersect). Considering the sequence of the torsion angles in **L12** (Table 1), four corners in the [12]aneNS$_3$ unit are present at the N and S donor atoms. Each pair of corners is separated by one −N−CH$_2$−CH$_2$−S− or −S−CH$_2$−CH$_2$−S− side-moiety unit featuring an *anti*-torsion angle at the C−C bond. Therefore, the conformation adopted by the macrocyclic unit in **L12** is [3333], according to the Dale convention, with the lone pairs (LPs) of electrons on the donor atoms in *exo*-dentate positions (i.e., pointing out of the ring cavity).
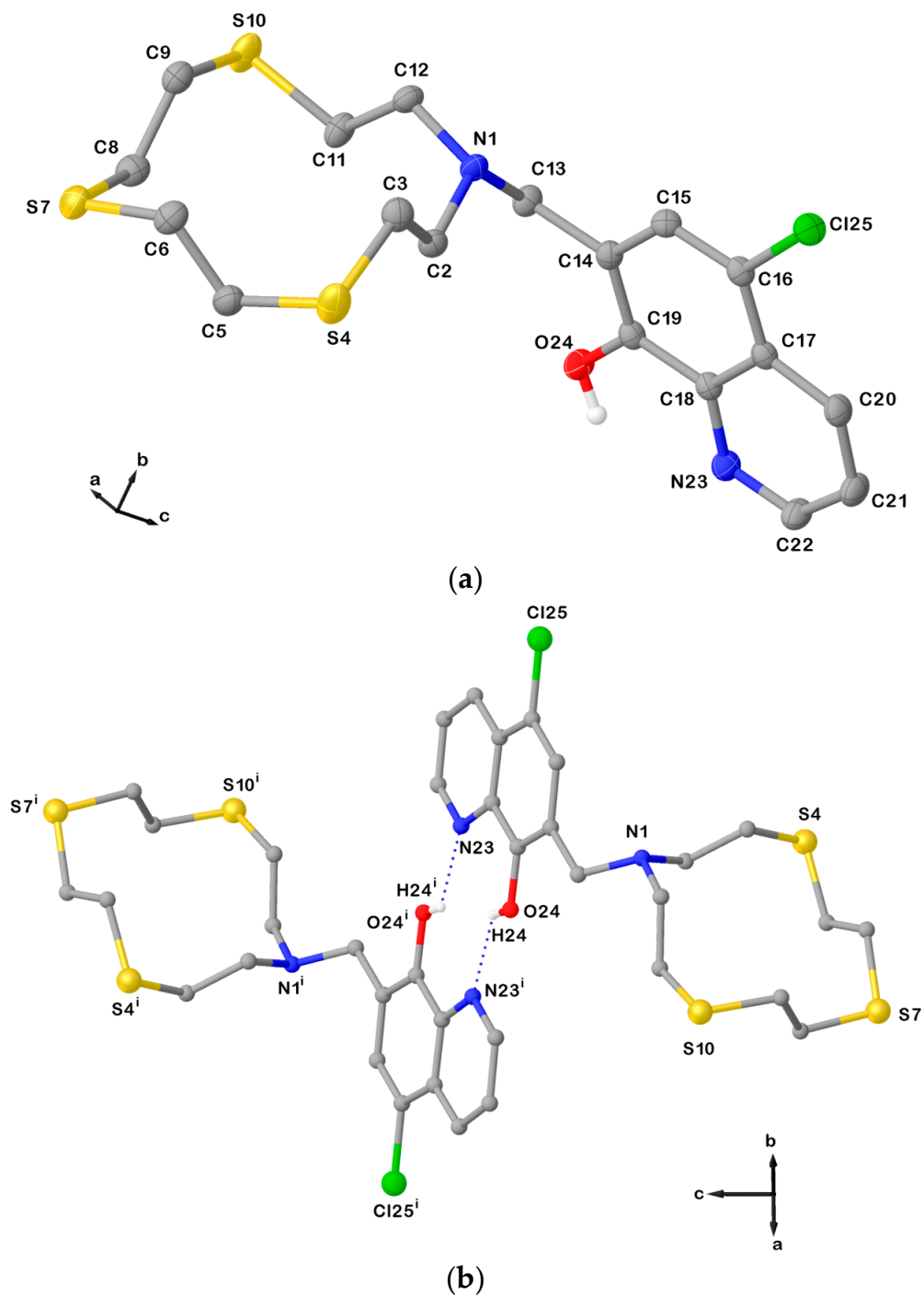
(**a**)

(**b**)

Figure 3. (**a**) View of the asymmetric unit of **L12** with the atom-labelling scheme adopted. Hydrogen atoms are omitted for clarity. Displacement ellipsoids are drawn at 50% probability level; (**b**) H-bonded dimeric arrangement found in **L12** with the numbering scheme adopted. Only interacting hydrogen atoms are shown for clarity. N23···O24^i = 2.8514(6) Å; O24^i−H24^i···N23 = 135°; and symmetry operation: i = −x, −y, 2−z. For selected bond lengths (Å) and angles (°), see Table S2 in the Supplementary Materials.

Table 1. Torsion angles (°) for the [12]aneNS₃ moieties in **L12**, **L20,** and **L21**·CHCl₃ with the Dale conformations in bracket squares (*gauche* torsion angles in red).

	L12 [3333]	L20 [11334]	L21·CHCl₃ [3333]
N1−C2−C3−S4	−172.90(14)	−66.0(3)	172.32(9)
C2−C3−S4−C5	77.12(18)	88.4(3)	−74.74(12)
C3−S4−C5−C6	75.95(19)	74.0(3)	−72.83(12)
S4−C5−C6−S7	−168.74(13)	175.40(17)	170.11(8)
C5−C6−S7−C8	65.4(2)	59.4(3)	−70.10(12)
C6−S7−C8−C9	67.8(2)	63.3(3)	−68.69(12)
S7−C8−C9−S10	−173.99(13)	−166.01(19)	173.80(8)
C8−C9−S10−C11	73.4(2)	68.5(3)	−70.48(12)
C9−S10−C11−C12	75.6(2)	66.8(3)	−75.57(12)
S10−C11−C12−N1	−165.24(17)	−155.5(2)	166.58(10)
C11−C12−N1−C2	64.8(3)	166.2(3)	−67.18(6)
C12−N1−C2−C3	69.1(2)	−73.8(4)	−69.40(5)

This type of conformation with *exo*-dentate donor atoms positioned at the corners is very common in medium and large aliphatic thioether macrocycles, as demonstrated by diffraction studies [26–28]: an *anti*-torsion angle at the C−C bond in the −S−CH₂−CH₂−S− units is preferred as a consequence of the repulsive 1,4-interaction between the sulfur LPs in a *gauche* arrangement [29]. On the other hand, a *gauche* torsion angle at the C−S bond in a −CH₂−CH₂−S−CH₂− sequence is not disfavored by the 1,4-interactions of the methylene protons, which lie beyond the sum of the corresponding van der Waals radii [30]. An opposite trend is observed in oxa-macrocycles due to the different C−O bond length and covalent radius of the donor atom [31].

In general, and in the specific case of **L12**, metal complexation or the involvement of one of the donor atoms of the [12]aneNS₃ unit in interactions with functionalities present in the pendant arms can strongly affect the conformation adopted by the macrocyclic unit in the solid state.

In fact, the X-ray crystal structure of **L20** is also characterized by dimeric arrangements via C−Br···S halogen bonds (XBs) involving one of the S donors from the macrocyclic unit as an XB acceptor, and the Br atom on the benzylic pendant arm as an XB donor (Figure 4).
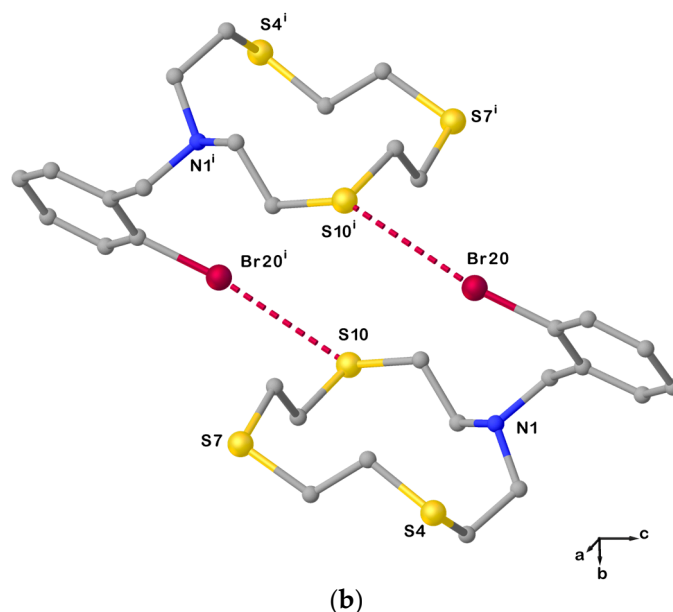

(**a**)

Figure 4. *Cont.*

(b)
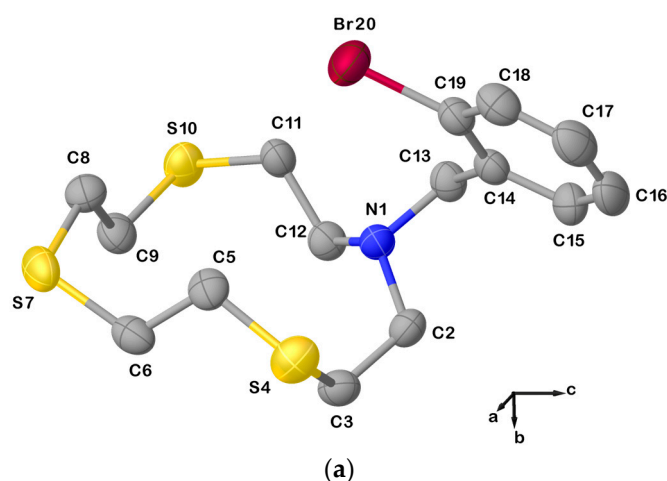
Figure 4. (**a**) View of the asymmetric unit of **L20** with the atom-labelling scheme adopted. Hydrogen atoms have been omitted for clarity. Displacement ellipsoids are drawn at 50% probability level; (**b**) X-bonded dimeric arrangement found in **L20** with the numbering scheme adopted. S10···Br20^i = 3.5030(3) Å; C19−Br20···S10^i = 163.6(1)°; and symmetry operation: i = −x, 1−y, −z. For selected bond lengths (Å) and angles (°), see Table S3 in the Supplementary Materials.

Due to this intermolecular interaction, the macrocyclic unit assumes a [11334] conformation as five corners can be identified in the cyclic structure (three consecutive at the atoms C2, C3, and S4, and the other two at S7 and S10, Table 1). Compared to **L12**, *anti*-torsion angles in **L20** remain at the C−C bonds in the sequences S4−C5−C6−S7, S7−C8−C9−S10, and S10−C11−C12−N1 (Table 1), while the torsion angles at the C2−C3 and C12−N1 bonds in the sequences N1−C2−C3−S4 and C11−C12−N1−C2 adopt a *gauche* and an *anti*-conformation, respectively (vice versa in the case of **L12**, Table 1). Presumably, the pulling effect of the bromine atom on the sulfur atom S10 in forming the XB causes the torsion angle at one of the C−N to change from a *gauche* to an *anti*-conformation, and the torsion angle at the C2−C3 bond to do the exact opposite.

This does not happen in the structure of **L21**·CHCl$_3$, in which it is the N atom from the macrocyclic unit that is involved in a weak intramolecular interaction with a functional group in the pendant arm. In fact, the conformation adopted by the [12]aneNS$_3$ unit in **L21**·CHCl$_3$ is again square-shaped [3333] with the *exo*-dentate donor atoms at the corners and −N−CH$_2$−CH$_2$−S− or −S−CH$_2$−CH$_2$−S− sequences with *anti*-torsion angles at the C−C bonds at the sides (Table 1). In this compound, an intramolecular HB is formed between the hydroxyl −OH function and the tertiary N donor from the macrocyclic unit (Figure 5a), which keeps the *exo*-dentate orientation of the LP in the HB interaction. Furthermore, dimeric arrangements are determined by C−H···O HBs involving one oxygen atom from the nitro group and one benzylic hydrogen atom (Figure 5b).
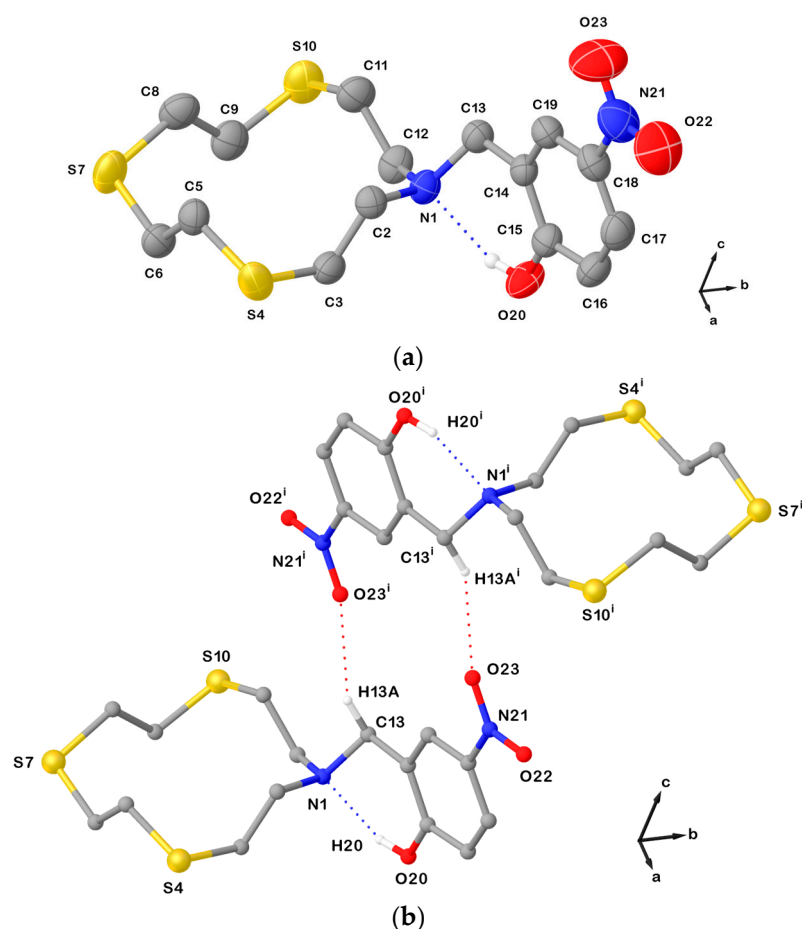
Figure 5. (**a**) View of the asymmetric unit in **L21**·CHCl$_3$ with the atom-labelling scheme adopted. Displacement ellipsoids are drawn at 50% probability level. Hydrogen atoms and the co-crystallized CHCl$_3$ molecule are omitted for clarity; (**b**) H-bonded dimeric arrangement found in **L21**·CHCl$_3$. Only interacting hydrogen atoms are shown for clarity. N1···O20 = 2.612(3); N1···H20 = 1.90(3) Å; O20−H20···N1 = 150(3)°; C13−O23^i = 3.354(3) Å; and symmetry operation: i = 1−*x*, 2−*y*, 2−*z*. For selected bond lengths (Å) and angles (°), see Table S4 in the Supplementary Materials.

A survey in the CSD (accessed on 13 January 2023) reveals a total of 31 X-ray crystal structures of [12]aneNS$_3$ (**L**) derivatives bearing functionalized pendant arms being reported either as free ligands or as metal complexes. The comparative analysis of the conformations assumed by the macrocyclic framework in the crystallographically independent 43 units (Table S5 in the Supplementary Materials) in terms of Dale notation shows that all reported free ligands (8 independent units) feature the [3333] conformation with the *exo*-dentate donor atoms at the corners (black asterisks in Figure 6a) which is in line with what is found in the structures of **L12** and **L21**·CHCl$_3$. The only exception is represented by the structure of **L20** mentioned above, and by the conformation assumed by the macrocycle in its bromide salt [H**L**]Br·2H$_2$O [1]. In this compound, the macrocycle is protonated at the secondary nitrogen atom and it assumes an unusual [84] (Table S5) conformation with only two corners, both at the carbon atoms, due to the intramolecular N−H···S HB involving the sulfur atom in front of the protonated N donor.
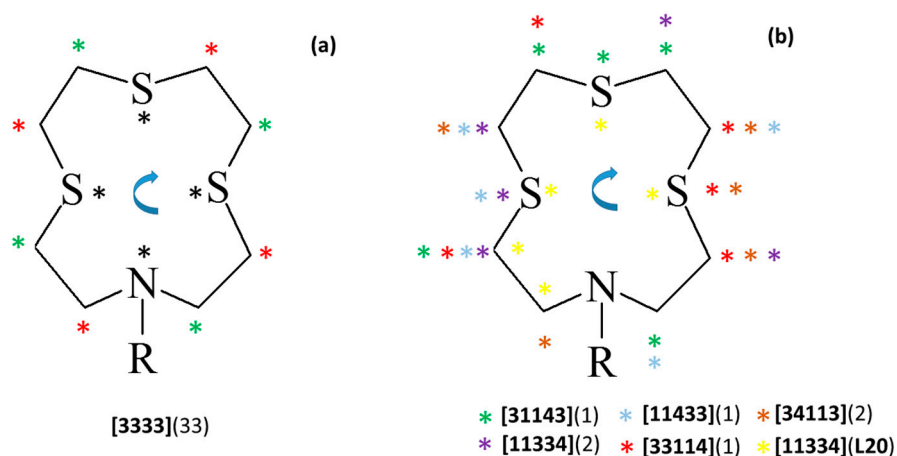
Figure 6. Schematic representation of the conformations adopted by the [12]aneNS$_3$ (**L**) macrocyclic moiety in the 31 X-ray crystal structures (43 independent units) retrieved from the CSD (Table S5 in the Supplementary Materials) featuring **L** derivatives (Figure 1) and their metal complexes. Asterisks indicate the corners in the various conformations according to the Dale notation. (**a**) Corner positions observed in [3333] conformations: black asterisks refer to the corner positions observed in free ligands, while red and green asterisks identify the corner positions observed in ligands coordinated to metal centers, and numbers in round brackets represent the overall number of independent units having the [3333] conformation; (**b**) corner positions in the alternative conformations observed in metal complexes of **L** derivatives, with each type of conformation identified by a different color of asterisk. The [84] conformation is not represented. To determine the number of bonds between each pair of corners and thereby assign the Dale notation to each conformation observed, start from the first corner to the left of the N atom as shown in the picture and proceed clockwise. This method was chosen to best illustrate the differences between conformations. The Dale notation is conventionally defined with the low numbers (i.e., the shortest edges) specified first, disregarding clockwise/anti-clockwise direction and crystallographic symmetries. In this way, all the conformations in Figure 6b would be assigned as [11334].

Among the remaining structures in which the macrocyclic moiety is involved in metal coordination, 25 independent units still display the macrocyclic moiety in a [3333] conformation with the corners located on carbon atoms and the donor atoms on –CH$_2$–CH$_2$–E–CH$_2$– (red asterisks in Figure 6a) or –CH$_2$–E–CH$_2$–CH$_2$– (green asterisks in Figure 6a, counting clockwise from the first corner to the left of the N atom as shown in Figure 6) side edges of the square-shaped conformation (E = N or S). A small number of compounds feature a conformation of the metal-coordinated macrocyclic unit in which three corners are located on three consecutive atoms including a S atom in the middle (purple, cyan, green, red, and brown asterisks in Figure 6b, see Table S5). Only in the case of **L20** does the sequence of three consecutive corners feature a S atom at the end of the three consecutive atoms involved (yellow asterisks in Figure 6b). Interestingly, no conformations with three consecutive corners involving N as one of the three consecutive atoms are known. Finally, only two structures are known in which the macrocyclic framework adopts a [84] conformation featuring only two corners (both at the same carbon atoms, Table S5), namely [H**L**]Br·2H$_2$O [1] and [CuCl(**L14**)]CuCl$_4$ [12].

4. Conclusions

The extent to which a macrocyclic ligand must pre-organize its conformation prior to complexation is one of the structural factors that can strongly affect the stability of the resulting metal complexes. For some macrocycles, the most stable conformation in the free state is not the most suitable to bind the metal ion and some changes are necessary to satisfy the stereochemical requirements of the complexation process. Herein, we have analyzed the conformation adopted in the solid state by the [12]aneNS$_3$ macrocyclic ring in

all its functionalized pendant arm derivatives, both as free ligands and as metal complexes. The derivatives of this 12-membered tetradentate NS_3 macrocycle in their free state adopt a [3333] conformation, regardless of the nature of the functional groups in the pendant arms, with all 4 donor atoms at the corners of a square-shaped structure with the lone pairs in *exo*-dentate positions. This is also confirmed by the X-ray crystal structures of **L12** and **L21**·$CHCl_3$ presented herein. Therefore, upon complexation, a drastic conformational change is required to bring the lone pairs on the donor atoms into *endo*-dentate arrangements to maximize coordination to the metal ion. The most commonly observed conformation of the [12]aneNS_3 moiety bound to metal ions is still of the type [3333], but the donor atoms sacrifice their preferred corner positions and each becomes part of a "side" of the square-shaped structure, with each side made up of a sequence of *gauche- anti-gauche* torsion angles. In very few reported cases, *endo*-dentate arrangements of the donor atoms in the [12]aneNS_3 moiety are reached upon coordination by assuming conformations that are different from the [3333]. These conformations of the type [33114] (or related ones by cyclic permutations of the corner positions, see Figure 6 and Figure S2 in the Supplementary Materials) all feature three consecutive corners, i.e., three consecutive atoms at which two *gauche* torsion angles intersect, of which a S atom is always in the middle. The other three donor atoms (two S and one N) are not in corner positions. A similar conformation of the [12]aneNS_3 moiety, but with a S donor atom being a terminal corner in the sequence of three consecutive ones (Figure 6b), has been observed in the structure of the free ligand **L20**, and it is determined by an intermolecular C−Br···S halogen bond. In **L20**, the conformation adopted by the macrocyclic unit is [11334] and not [3333] as normally observed; the three S donor atoms are all in corner positions while the N donor atom is not and is characterized by an *endo*-dentate orientation of its lone pair. We conclude that this is the only case in which the functional group in the pendant arm affects the conformation assumed by the [12]aneNS_3 macrocyclic moiety due to a direct intermolecular interaction with one of the S donor atoms. Our results suggest that in order to have a conformation other than [3333] for the macrocyclic moiety of uncoordinated pendant arm derivatives of **L**, rather than considering intramolecular HBs involving the N atom and HB donors in the pendant arms (see the structure of **L21**·$CHCl_3$), it is more convenient to look for functionalities that can interact with the S donors of the macrocyclic moiety.

Conflicts of Interest: The authors declare no conflict of interest.

References

1.　Glenny, M.W.; van de Water, L.G.A.; Vere, J.M.; Blake, A.J.; Wilson, C.; Driessen, W.L.; Reedijk, J.; Schröder, M. Improved synthetic methods to mixed-donor thiacrown ethers. *Polyhedron* **2006**, *25*, 599–612. [CrossRef]

2.　Glenny, M.W.; van de Water, J.M.; Driessen, W.L.; Reedijk, J.; Blake, A.J.; Wilson, C.; Schröder, M. Conformational and stereochemical flexibility in cadmium(II) complexes of aza-thioether macrocycles. *Dalton Trans.* **2004**, *13*, 1953–1959. [CrossRef] [PubMed]

3.　Donamaría, R.; Lippolis, V.; López-de-Luzuriaga, J.M.; Monge, M.; Nieddu, M.; Olmos, M.E. Tuning Au(I)···Tl(I) Interactions via Mixed Thia-Aza Macrocyclic Ligands: Effects in the Structural and Luminescence Properties. *Inorg. Chem.* **2017**, *56*, 12551–12563. [CrossRef]

4.　Donamaría, R.; Lippolis, V.; López-de-Luzuriaga, J.M.; Monge, M.; Nieddu, M.; Olmos, M.E. Influence of the Number of Metallophilic Interactions and Structures on the Optical Properties of Heterometallic Au/Ag Complexes with Mixed-Donor Macrocyclic Ligands. *Inorg. Chem.* **2018**, *57*, 11099–11112. [CrossRef]

5.　Habata, Y.; Noto, K.; Osaka, F. Substituents Effects on the Structures of Silver Complexes with Monoazatrithia-12-Crown-4 Ethers Bearing Substituted Aromatic Rings. *Inorg. Chem.* **2007**, *46*, 6529–6534. [CrossRef] [PubMed]

6.　Hodorogea, A.M.; Silvestru, A.; Lippolis, V.; Pop, A. Group 12 metal complexes of mixed thia/aza and thia/oxa/aza macrocyclic ligands. *Polyhedron* **2022**, *216*, 115650. [CrossRef]

7.　Ogawa, T.; Koike, K.; Matsumoto, J.; Kajita, Y.; Masuda, H. Synthesis and characterization of tricarbonyl-molybdenum complexes bearing monoaza-trithia-macrocyclic ligands. *Inorg. Chim. Acta* **2013**, *401*, 101–106. [CrossRef]

8.　Habata, Y.; Osaka, F. Dimetallo[3.3]para- and metacyclophanes by self-assembly of pyridylmethyl armed-monoazatrithia- and monoazadithiaoxa-12-crown-4 ethers with Ag$^+$. *Dalton Trans.* **2006**, *15*, 1836–1841. [CrossRef]

9.　Aragoni, M.C.; Arca, M.; Bencini, A.; Caltagirone, C.; Garau, A.; Isaia, F.; Light, M.E.; Lippolis, V.; Lodeiro, C.; Mameli, M.; et al. Zn^{2+}/Cd^{2+} optical discrimination by fluorescent chemosensors based on 8-hydroxyquinoline derivatives and sulfur-containing macrocyclic units. *Dalton Trans.* **2013**, *42*, 14516–14530. [CrossRef]

10.　Bazzicalupi, C.; Caltagirone, C.; Cao, Z.; Chen, Q.; Di Natale, C.; Garau, A.; Lippolis, V.; Lvova, L.; Liu, H.; Lundström, I.; et al. Multimodal Use of New Coumarin-Based Fluorescent Chemosensors: Towards Highly Selective Optical Sensors for Hg^{2+} Probing. *Chem. Eur. J.* **2013**, *19*, 14639–14653. [CrossRef]

11.　Aragoni, M.C.; Arca, M.; Bencini, A.; Blake, A.J.; Caltagirone, C.; Decortes, A.; Demartin, F.; Devillanova, F.A.; Faggi, E.; Dolci, L.S.; et al. Coordination Chemistry of *N*-aminopropyl pendant arm derivatives of mixed N/S-, and N/S/O-donor macrocycles, and construction of selective fluorimetric chemosensors for heavy metal ions. *Dalton Trans.* **2005**, *18*, 2994–3004. [CrossRef]

12.　Love, J.B.; Vere, J.M.; Glenny, M.W.; Blake, A.J.; Schröder, M. Ditopic azathioethers macrocycles as hosts for transition metal salts. *Chem. Commun.* **2001**, 2678–2679. [CrossRef]

13.　Glenny, M.W.; Lacombe, M.; Love, J.B.; Blake, A.J.; Lindoy, L.F.; Luckay, R.C.; Gloe, K.; Antonioli, B.; Wilson, C.; Schröder, M. Design and synthesis of heteroditopic aza-thioether macrocycles for metal extraction. *New J. Chem.* **2006**, *30*, 1755–1767. [CrossRef]

14.　Hoover, L.R.; Pryor, T.; Weitgenant, J.A.; Williams, P.E.; Storhoff, B.N.; Huffman, J.C. 4′ Diphenylphosphino and bromo derivatives of 10-phenyl-1,4,7-trithia-10-aza-cyclododecane 4-R-C$_6$H$_4$N(CH$_2$CH$_2$S)$_2$CH$_2$CH$_2$SCH$_2$CH$_2$. *Phosphorus Sulfur Silicon Relat. Elem.* **1997**, *122*, 155–166. [CrossRef]

15.　Habata, Y.; Seo, J.; Otawa, S.; Osaka, F.; Noto, K.; Lee, S.S. Synthesis of diazahexathia-24-crown-8 derivatives structures of Ag$^+$ complexes. *Dalton Trans.* **2006**, *18*, 2202–2206. [CrossRef] [PubMed]

16.　Masuri, S.; Cadoni, E.; Cabiddu, M.G.; Isaia, F.; Demuru, M.G.; Moráň, L.; Buček, D.; Vaňhara, P.; Havel, J.; Pivetta, T. The first copper(II) complex with 1,10-phenanthroline and salubrinal with interesting biochemical properties. *Metallomics* **2020**, *12*, 891–901. [CrossRef]

17.　Strohalm, M.; Kavan, D.; Novak, P.; Volný, M.; Havlíček, V. mMass 3: Cross-platform Software Environment for Precise Analysis of Mass Spectrometric Data. *Anal. Chem.* **2010**, *82*, 4648–4651. [CrossRef]

18.　*SAINT*, Version 6.36a; Bruker AXS Inc.: Fitchburg, WI, USA, 2002.

19.　*SMART*, Version 5.624; Bruker AXS Inc.: Fitchburg, WI, USA, 2001.

20.　Altomare, A.; Cascarano, G.; Giacovazzo, C.; Guagliardi, A.; Burla, M.C.; Polidori, G.; Camalli, M. SIR92—A program for automatic solution of crystal structures by direct methods. *J. Appl. Crystallogr.* **1994**, *27*, 435–436. [CrossRef]

21.　*CrysAlisPro*, Version 1.171.37.35; Agilent Technologies: Oxfordshire, UK, 2014; Release 13-08-2014 CrysAlis171.NET.

22.　Sheldrick, G.M. SHELXT—Integrated Space-Group and Crystal-Structure Determination. *Acta Crystallogr. Sect. A* **2015**, *71*, 3–8. [CrossRef]

23.　Sheldrick, G.M. Crystal Structure Refinement with SHELXL. *Acta Crystallogr. Sect. C* **2015**, *71*, 3–8. [CrossRef]

24.　Dolomanov, O.V.; Bourhis, L.J.; Gildea, R.J.; Howard, J.A.K.; Puschmann, H. OLEX2: A Complete Structure Solution, Refinement and Analysis Program. *J. Appl. Crystallogr.* **2009**, *42*, 339–341. [CrossRef]

25.　Dale, J. Exploratory Calculations of Medium and Large Rings. *Acta Chem. Scand.* **1973**, *27*, 1115–1129. [CrossRef]

26.　Simone, R.E.; Glick, M.D. Structures of the macrocyclic polythiaether 1,4,8,11-tetrathiacyclotetradecane and implications for transition-metal chemistry. *J. Am. Chem. Soc.* **1976**, *98*, 762–767.

27. Riley, D.P.; Oliver, J.D. Synthesis and crystal structure of a novel rhodium(I) complex of an inside-out hexathia crown ether. *Inorg. Chem.* **1983**, *22*, 3361–3363. [CrossRef]

28. Blake, A.J.; Gould, R.O.; Halcrow, M.A.; Schröder, M. Conformational studies on [16]aneS$_4$. Structures of α- and β-[16]aneS$_4$ ([16]aneS$_4$ = 1,5,9,13-tetrathiacyclohexadecane). *Acta Crystallogr. Sect. B* **1993**, *49*, 773–779. [CrossRef]

29. Wolf, R.E.; Hartman, J.-A.R.; Storey, J.M.E.; Foxman, B.M.; Cooper, S.R. Crown thioether chemistry: Structural and conformational studies of tetrathia-12-crown-4, pentathia-15-crown-5, and hexathia-18-crown-6. Implications for ligand design. *J. Am. Chem. Soc.* **1987**, *109*, 4328–4335. [CrossRef]

30. Bovil, M.J.; Chadwick, D.J.; Sutherland, I.O. Molecular mechanics calculations for ethers. The conformations of some crown ethers and the structure of the complex of 18-crown-6 with benzylammonium thiocyanate. *J. Chem. Soc. Perkin Trans.* **1980**, *2*, 1529–1543. [CrossRef]

31. Mark, J.E.; Flory, P.J. The Configuration of the Polyoxyethylene Chain. *J. Am. Chem. Soc.* **1965**, *87*, 1415–1423. [CrossRef]